



**HAL**  
open science

# Formation and Possible Reactions of Organometallic Intermediates with Active Copper(I) Catalysts in ATRP

Kristin Schröder, Dominik Konkolewicz, Rinaldo Poli, Krzysztof Matyjaszewski

► **To cite this version:**

Kristin Schröder, Dominik Konkolewicz, Rinaldo Poli, Krzysztof Matyjaszewski. Formation and Possible Reactions of Organometallic Intermediates with Active Copper(I) Catalysts in ATRP. *Organometallics*, 2012, 31 (22), pp.7994-7999. 10.1021/om3006883 . hal-03157764

**HAL Id: hal-03157764**

**<https://hal.science/hal-03157764>**

Submitted on 3 Mar 2021

**HAL** is a multi-disciplinary open access archive for the deposit and dissemination of scientific research documents, whether they are published or not. The documents may come from teaching and research institutions in France or abroad, or from public or private research centers.

L'archive ouverte pluridisciplinaire **HAL**, est destinée au dépôt et à la diffusion de documents scientifiques de niveau recherche, publiés ou non, émanant des établissements d'enseignement et de recherche français ou étrangers, des laboratoires publics ou privés.

**Formation and Possible Reactions of Organometallic Intermediates with Active Copper(I) Catalysts in ATRP**

Journal:	<i>Organometallics</i>
Manuscript ID:	om-2012-006883.R1
Manuscript Type:	Article
Date Submitted by the Author:	26-Oct-2012
Complete List of Authors:	Matyjaszewski, Krzysztof; Carnegie Mellon University, Department of Chemistry Konkolewicz, Dominik; Carnegie Mellon University, Chemistry Schröder, Kristin; Carnegie Mellon University, Chemistry Poli, Rinaldo; CNRS, Laboratoire de Chimie de Coordination

SCHOLARONE™  
Manuscripts

1  
2  
3  
4  
5  
6  
7  
8  
9  
10  
11  
12  
13  
14  
15  
16  
17  
18  
19  
20  
21  
22  
23  
24  
25  
26  
27  
28  
29  
30  
31  
32  
33  
34  
35  
36  
37  
38  
39  
40  
41  
42  
43  
44  
45  
46  
47  
48  
49  
50  
51  
52  
53  
54  
55  
56  
57  
58  
59  
60

# Formation and Possible Reactions of Organometallic Intermediates with Active Copper(I) Catalysts in ATRP

*Kristin Schröder, Dominik Konkolewicz, Rinaldo Poli,<sup>†‡</sup> and Krzysztof Matyjaszewski\**

Department of Chemistry, Carnegie Mellon University, 4400 Fifth Avenue, Pittsburgh,  
Pennsylvania 15213, USA

<sup>†</sup>Laboratoire de Chimie de Coordination (LCC), CNRS, Université de Toulouse; UPS, INPT,  
205, route de Narbonne, 31077 Toulouse, France

<sup>‡</sup>Institut Universitaire de France, 103, bd Saint-Michel, 75005 Paris, France

*KEYWORDS: Controlled Radical Polymerization, ATRP, organometallic mediated radical polymerization (OMRP), Catalytic Chain Transfer (CCT), Catalytic Radical Termination (CRT), TPMA.*

ABSTRACT: The Cu<sup>I</sup> complex obtained in situ from Cu<sup>I</sup> and tris((4-methoxy-3,5-dimethylpyridin-2-yl)-methyl)amine (TPMA\*) is currently the most reducing and the most active catalyst for atom transfer radical polymerizations (ATRP). The complex has a high affinity for alkyl halides (ATRP pathway) but also has sufficient affinity towards organic radicals to potentially participate in organometallic mediated radical polymerization (OMRP).

1  
2  
3 Thus, the radical polymerization of *n*-butyl acrylate initiated by AIBN (azobisisobutyronitrile)  
4 was significantly retarded and the molecular weights decreased in the presence of the  
5  
6  
7  
8  $\text{Cu}^{\text{I}}/\text{TPMA}^*$  complex. These results suggest the presence of a Cu-mediated termination  
9  
10 processes, even after the amount of radicals generated from AIBN exceeded the initial amount of  
11  
12  $\text{Cu}^{\text{I}}/\text{TPMA}^*$ . Nevertheless, in the presence of alkyl bromides, which act as ATRP initiators for  
13  
14 acrylates, control was gained through metal mediated halogen atom transfer, *i.e.* ATRP, not  
15  
16 OMRP.  
17  
18  
19  
20  
21  
22

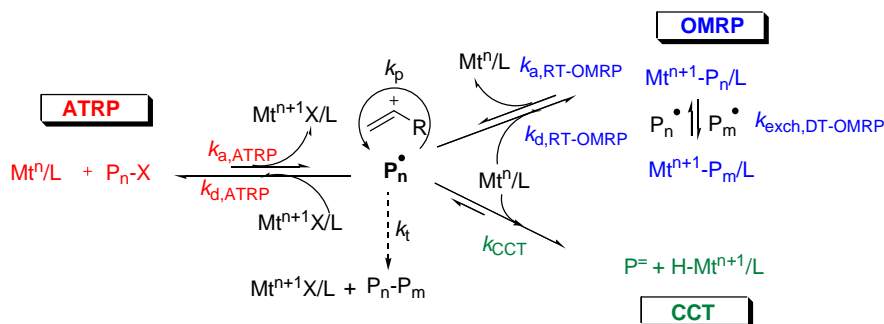
### 23 ***Introduction***

24  
25 Conventional radical polymerization (RP) procedures are the most commonly employed  
26  
27 industrial techniques for the production of commodity polymers.<sup>1</sup> RP is characterized by a  
28  
29 tolerance to functional groups and many impurities, but provides poor control over polymer  
30  
31 architecture, molecular weight ( $M_n$ ) and molecular weight distribution ( $M_w/M_n$ ). In contrast,  
32  
33 reversible-deactivation radical polymerizations (RDRP),<sup>2</sup> also named controlled/living radical  
34  
35 polymerizations (CRP), can provide control over  $M_n$ ,  $M_w/M_n$ , and access to polymers with  
36  
37 predefined functionalities, compositions, and architectures.<sup>3</sup> Transition metal-mediated RDRP  
38  
39 techniques include atom transfer radical polymerization (ATRP)<sup>4</sup> and organometallic mediated  
40  
41 radical polymerization (OMRP).<sup>5</sup> They rely on a dynamic equilibrium between a low fraction of  
42  
43 growing radicals and a predominant fraction of dormant species.  
44  
45  
46  
47

48 Since the pioneering work on OMRP by Wayland and co-workers, utilizing cobalt porphyrin  
49  
50 complexes for the polymerization of acrylates,<sup>6</sup> the procedure has been expanded to employ  
51  
52 various complexes based on a range of transition metals; *e.g.* titanium, chromium, iron, cobalt  
53  
54 and others,<sup>7</sup> for a large number of monomers, including vinyl acetate<sup>8</sup> and acrylamides.<sup>9, 10</sup>  
55  
56 OMRP utilizes a fast reversible homolytic cleavage of a transition metal-carbon bond, Scheme 1.  
57  
58  
59  
60

OMRP reactions are often initiated by conventional organic radical sources, *e.g.* azobisisobutyronitrile (AIBN) in the presence of a transition metal complex in its lower oxidation state. The concentration of growing radical chains ( $P_n^*$ ) is controlled by a formal reversible one electron process, in which  $P_n^*$  reacts with a redox-active transition metal complex ( $Mt^{n+1}L$ ), resulting in formation of an oxidized organometallic complex ( $Mt^{n+1}-P_n/L$ ) in the so-called reversible termination process (RT OMRP). The dynamic active/dormant species equilibrium, strongly favoring the dormant state, *i.e.*  $Mt^{n+1}-P_n/L$ , should ensure a low constant concentration of propagating radicals ( $P_n^*$ ), allowing a concurrent growth of all polymer chains and minimizing bimolecular termination reactions. Additional control may be provided through a degenerative transfer process (DT OMRP) which involves the reversible associative exchange between  $Mt^{n+1}-P_n/L$  and another propagating radical ( $P_m^*$ ), releasing the previous dormant radical ( $P_n^*$ ).<sup>8a</sup> Consequently, in an OMRP all resulting dormant polymer chains are metal-capped, therefore OMRP requires the presence of stoichiometric amounts of  $Mt^{n+1}L$ .

In some cases, catalytic chain transfer (CCT) reactions, Scheme 1, may be involved, especially when using cobalt as the transition metal for the polymerization of methacrylates.<sup>8b, 11</sup> Formally,  $\beta$ -hydrogen transfer ( $k_{CCT}$ ) between  $P_n^*$  and  $Mt^{n+1}L$  yields an olefin-terminated species ( $P^-$ ) and a metal hydride complex,  $H-Mt^{n+1}L$ . The  $H-Mt^{n+1}L$  complex reinitiates polymerization of a vinyl monomer forming  $Mt^{n+1}L$  and a propagating radical.



**Scheme 1.** Schematic illustration of ATRP and OMRP pathways.

1  
2  
3 In contrast to OMRP, ATRP gives halogen-capped polymers and is controlled by a fast and  
4 reversible homolytic cleavage of a C-halogen bond in a redox reaction with a transition metal  
5 catalyst, Scheme 1, with  $K_{\text{ATRP}} = k_{\text{a,ATRP}}/k_{\text{d,ATRP}}$ .<sup>12</sup> Since ATRP is a true catalytic process the  
6 transition metal complex can be used in sub-stoichiometric concentrations. However, as is the  
7 case in OMRP and for the same reasons, the dynamic active/dormant species equilibrium must  
8 strongly favor the stable dormant state, in this case  $\text{P}_n\text{-X}$ . Recent developments in ATRP<sup>13</sup> *e. g.*,  
9 initiators for continuous activators regeneration (ICAR),<sup>14</sup> target the *in-situ* regeneration of the  
10 activator complex ( $\text{M}^{\text{n}}/\text{L}$ ), from the oxidatively stable deactivator complex ( $\text{M}^{\text{n}+1}\text{X}/\text{L}$ ), formed by  
11 unavoidable termination reactions. They allow the transition metal complex to be utilized at parts  
12 per million (ppm) concentrations.

13  
14  
15 Values of  $K_{\text{ATRP}}$  can vary over a wide range.<sup>15</sup> Simply altering the catalyst ( $\text{M}^{\text{n}}\text{L}$ ) or initiator  
16 ( $\text{R-X}$ ) structure provides a powerful tool to influence  $K_{\text{ATRP}}$ , in each case by more than six orders  
17 of magnitude.<sup>16</sup> Recently, active catalysts for ATRP were developed by incorporating electron  
18 donating groups into pyridine based ligand structures such as 2,2'-bipyridine (bpy)<sup>17</sup> and tris(2-  
19 pyridylmethyl)amine (TPMA) scaffolds.<sup>18</sup> Tris((4-methoxy-3,5-dimethylpyridin-2-yl)-methyl)-  
20 amine (TPMA\*) currently provides the most active ligand developed for Cu-catalyzed ATRP.

21  
22 Part of a quest to develop a deeper understanding of the mechanisms of transition metal  
23 mediated CRP has focused on the potential interplay between ATRP, OMRP, and CCT  
24 mechanisms.<sup>5a, 7b</sup> ATRP and OMRP can interact synergistically (*i.e.* the two equilibria, each  
25 providing complementary control over the concentration of the propagating radicals) since the  
26 ATRP catalyst in the low oxidation state may also act as an OMRP radical trap. Examples of  
27 such systems include Mo-mediated,<sup>19</sup> and Os-mediated<sup>20</sup> polymerizations conducted with  
28 phosphine containing complexes. However, if the equilibria are too strongly displaced towards  
29  
30  
31  
32  
33  
34  
35  
36  
37  
38  
39  
40  
41  
42  
43  
44  
45  
46  
47  
48  
49  
50  
51  
52  
53  
54  
55  
56  
57  
58  
59  
60

1  
2  
3 the dormant species, then the one-electron oxidative addition between  $Mt^n/L$  and  $R-X$  leading to  
4  
5  $Mt^{n+1}-X/L$  and  $Mt^{n+1}-R/L$  becomes irreversible and, essentially, no polymerization takes place.  
6  
7

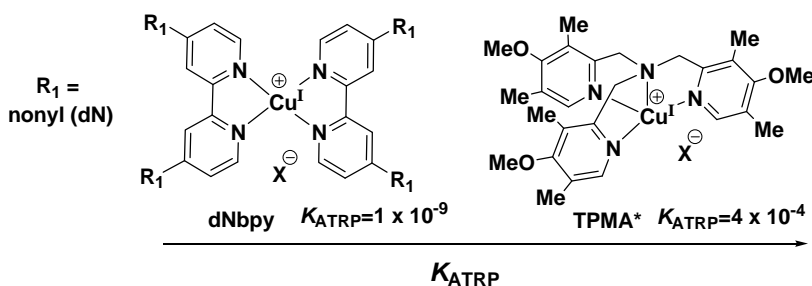
8 OMRP and CCT may competitively interplay, because both processes involve the same  
9  
10 reagents  $Mt^n/L$  and  $P_n^*$ . The first one leads to reversible metal-carbon bond formation and the  
11  
12 second one to  $\beta$ -H atom transfer. The former process can also include  $\beta$ -H elimination from the  
13  
14 OMRP dormant species  $Mt^{n+1}-P_n/L$  to yield the same product as in CCT. Such reactions were  
15  
16 reported for Mo-mediated polymerizations<sup>19a</sup> and Fe-mediated processes with  $\alpha$ -diimine<sup>21</sup> or  
17  
18 amine-bis(phenolate) ligands.<sup>22</sup>  
19  
20

21  
22 For Cu-catalyzed ATRP processes, only one report in 1998 pointed to the possibility of an  
23  
24 interaction between an organic radical and a copper(I) complex in the absence of halogen  
25  
26 atoms.<sup>23</sup> Diminished polymerization rates for methyl acrylate (MA) initiated by AIBN were  
27  
28 observed in the presence of  $Cu^IOTf$  complexes with alkyl-substituted bpy ligands. The  
29  
30 generation of sufficiently stabilized  $RCu^{II}$  dormant species is notable, since stable alkyl  
31  
32 derivatives of  $Cu^{II}$  are scarce.<sup>24</sup> The possibility of a  $\beta$ -H atom transfer process, leading to  $Cu^{II}-H$   
33  
34 intermediates has not yet been discussed.  
35  
36

37  
38 Herein, we investigated the role of  $Cu/TPMA^*$  complexes under ATRP (with  $R-X$ ) and OMRP  
39  
40 (with AIBN) conditions. After the initial evaluation of the effect of  $Cu/TPMA^*$  complexes on  
41  
42  $K_{ATRP}$  under ATRP conditions,<sup>18</sup> an examination of the effect of the complex under OMRP  
43  
44 conditions revealed a significant influence on polymerization rates and molecular weight  
45  
46 distributions. The unprecedented contribution of Cu complexes to catalyzed radical terminations  
47  
48 is subsequently critically evaluated.  
49  
50

## 51 52 53 54 ***Results & Discussion*** 55 56 57 58 59 60

**$K_{\text{ATRP}}$  and  $k_a$  for Cu/TPMA\*, Cu/dNbpy and Cu/bpy:** The values of  $K_{\text{ATRP}}$  and  $k_a$  for the Cu<sup>I</sup>/TPMA\* catalyst complex were determined *via* stopped-flow measurements using methyl 2-bromopropionate (MBP) as an initiator in acetonitrile at 25 °C.<sup>16</sup> A value for  $K_{\text{ATRP}}$  of  $4.2 \times 10^{-4}$  for Cu/TPMA\*<sup>18</sup> was determined from the modified Fischer equation<sup>25</sup> based on the persistent radical effect (PRE), cf. SI.<sup>26</sup> The value of  $K_{\text{ATRP}}$  obtained for Cu/TPMA\* is more than five orders of magnitude greater than that determined for Cu/dNbpy and six orders of magnitude greater than that measured for the unsubstituted Cu/bpy catalyst complex,  $K_{\text{ATRP}} = 1.0 \times 10^{-9}$  and  $K_{\text{ATRP}} = 1.3 \times 10^{-10}$ , respectively (Scheme 2).<sup>16</sup>



**Scheme 2.** Effect of ligands on  $K_{\text{ATRP}}$  in Cu-catalyzed ATRP processes under the same conditions (MBP, MeCN, 25°C).

An activation rate coefficient  $k_{a,\text{TPMA}^*} = 8400 \text{ M}^{-1}\text{s}^{-1}$  was determined by trapping the generated methyl 2-propionate radicals with 2,2,6,6-tetramethylpiperidyl-1-oxy (TEMPO). This value, in comparison with reported values<sup>16</sup> of  $k_{a,\text{dNbpy}} = 3.7 \times 10^{-2} \text{ M}^{-1}\text{s}^{-1}$  and  $k_{a,\text{bpy}} = 4.0 \times 10^{-3} \text{ M}^{-1}\text{s}^{-1}$ , correlated well with the trend observed for  $K_{\text{ATRP}}$ . The high activation rate coefficient, combined with the high equilibrium constant indicates that deactivation rate coefficient is sufficiently fast to provide good control in an ATRP ( $k_{d,\text{TPMA}^*} = 2 \times 10^7 \text{ M}^{-1}\text{s}^{-1}$ ).



1  
2  
3 **Normal ATRP and ICAR ATRP of acrylates with Cu/TPMA\* in the presence of an alkyl**  
4 **halide:** First, “normal” and ICAR ATRP were investigated to assess the viability of copper  
5 complexes formed with TPMA\* for the polymerization of acrylates. The high catalyst loadings  
6 in a “normal” ATRP, combined with the very high activity of Cu<sup>I</sup>/TPMA\*, initially created very  
7 high radical concentrations which resulted in significant termination reactions and relatively  
8 poor control. On the contrary, ICAR ATRP, which relies on continuous regeneration of low  
9 concentrations of Cu<sup>I</sup>/TPMA\*, showed excellent control over  $M_n$  with concentrations of catalyst  
10 as low as 100 ppm ( $M_w/M_n = 1.15$ ) down to 5 ppm ( $M_w/M_n = 1.43$ ), cf. SI Table S1 and Fig. S1.  
11 These findings agree with the results of PREDICI<sup>®</sup> simulations and indicate that very active  
12 ATRP complexes are better suited for low ppm ICAR ATRP, rather than normal ATRP.<sup>18</sup>  
13  
14  
15  
16  
17  
18  
19  
20  
21  
22  
23  
24  
25  
26  
27  
28

29 **OMRP initiated by AIBN in the presence of Cu<sup>I</sup>BF<sub>4</sub>/TPMA\* in the absence of an alkyl**  
30 **halide.** The very strongly reducing and active Cu<sup>I</sup>BF<sub>4</sub>/TPMA\* complexes could potentially  
31 directly interact with propagating radicals. First, control experiments with BA and AIBN under  
32 typical conventional radical polymerization conditions were performed and exhibited the  
33 expected uncontrolled behaviour with very fast kinetics and broad molecular weight distributions  
34  
35  
36  
37  
38  
39  
40  
41 ( $M_w/M_n \sim 20$ ) (Fig. 1 and 2A, green).  
42  
43  
44

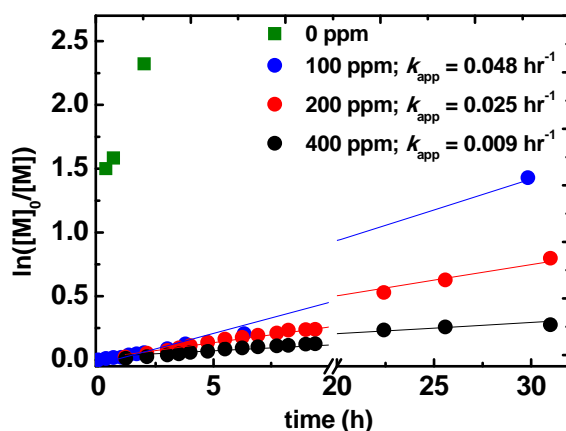


**Figure 1.** Kinetic plots for polymerization with various loadings of  $[\text{Cu}^{\text{I}}]$ ; conditions  $[\text{BA}]:[\text{AIBN}]:[\text{TPMA}^*]:[\text{Cu}^{\text{I}}(\text{CH}_3\text{CN})_4\text{BF}_4] = [160]:[0.2]:[0.06-0.24]:[0.016-0.064]$ ,  $[\text{BA}] = 5.6$  M, 20% (v/v) anisole,  $T = 60$  °C.

Then, a series of polymerizations of BA initiated by AIBN in the presence of various concentrations of the  $\text{Cu}^{\text{I}}\text{BF}_4/\text{TPMA}^*$  complex was carried out. The experiments with 100, 200 and 400 ppm  $\text{Cu}^{\text{I}}$  were repeated twice, and average values and standard deviation for the pseudo first order kinetic plots are presented in the SI, Tab. S2. In the presence of 100 ppm of  $\text{Cu}^{\text{I}}\text{BF}_4/\text{TPMA}^*$ , the rate of polymerization was much slower than in conventional radical polymerization. Conversion increased in a linear fashion in semilogarithmic coordinates and after nearly 30 h reached only 76 %, Fig.1 and SI Fig. S2A. Increasing the amount of  $\text{Cu}^{\text{I}}$  complex, to 200 ppm and then to 400 ppm (mol, vs. monomer), resulted in even slower reactions, reaching after 31 h only 55% and 25% monomer conversion, respectively. With  $[\text{AIBN}]:[\text{Cu}^{\text{I}}]$  ratio of 1:1, corresponding to 1250 ppm Cu (*i.e.* under typical OMRP conditions), the polymerization reached only ~2% after 45.8 h. Assuming a quantitative reaction between  $\text{Cu}^{\text{I}}$  and radicals generated from AIBN ( $f = 0.8$ ) to yield an  $\text{R-Cu}^{\text{II}}$  OMRP dormant species, complete consumption of  $\text{Cu}^{\text{I}}$  should occur after 1.6 h, 3.2 h, and 6.8 h for systems with 100 ppm  $\text{Cu}^{\text{I}}$  (5% AIBN consumption), 200 ppm (10%) and 400 ppm (20% AIBN consumption), respectively. This can be determined from the exponential decay in the AIBN concentration over time,  $[\text{AIBN}]_t = [\text{AIBN}]_0 \exp(-k_{\text{azo}}t)$ . Setting the loss of AIBN equal to the initial  $[\text{Cu}^{\text{I}}]$  gives the time (t) needed to react all  $\text{Cu}^{\text{I}}$ , *i.e.*  $[\text{Cu}^{\text{I}}]_0 = 2f ([\text{AIBN}]_0 - [\text{AIBN}]_t) = 2f [\text{AIBN}]_0 (1 - \exp(-k_{\text{azo}}t))$ ;

$$t = -\frac{1}{k_{\text{azo}}} \ln \left( 1 - \frac{[\text{Cu}^{\text{I}}]_0}{2f[\text{AIBN}]_0} \right).$$

However, nearly linear pseudo first-order kinetic plots were observed for more than 30 h, indicating a relatively constant amount of radicals in the system.

This observation confirms that a radical quenching process must operate not only in the presence of  $\text{Cu}^{\text{I}}/\text{TPMA}^*$  but also in the presence of the putative  $\text{R-Cu}^{\text{II}}/\text{TPMA}^*$  species. The progressive decrease of the apparent propagation rate constants:  $k_{\text{app},100\text{ppm}} = 0.049 \text{ h}^{-1}$ ,  $k_{\text{app},200\text{ppm}} = 0.017 \text{ h}^{-1}$ ,  $k_{\text{app},400\text{ppm}} = 0.008 \text{ h}^{-1}$  follows the amounts of  $\text{Cu}^{\text{I}}\text{BF}_4/\text{TPMA}^*$  (Table S2). In all cases there is a decrease in the rate that is proportional to the concentration of the  $\text{Cu}^{\text{I}}\text{BF}_4/\text{TPMA}^*$ , within the standard deviations of the 100, 200 and 400 ppm experiments. This suggests the possibility of radical trapping and/or a catalytic retardation process. It should be stressed that the  $k_{\text{app},100\text{ppm}}$  for  $\text{Cu}^{\text{I}}\text{BF}_4/\text{TPMA}^*$  was nearly eight times smaller than  $k_{\text{app}}$  of the ICAR ATRP reactions using the same amount of Cu and AIBN but in the presence of alkyl bromides (SI Table S1, entry 5,  $k_{\text{app},100\text{ppm}} = 0.36 \text{ h}^{-1}$ ).

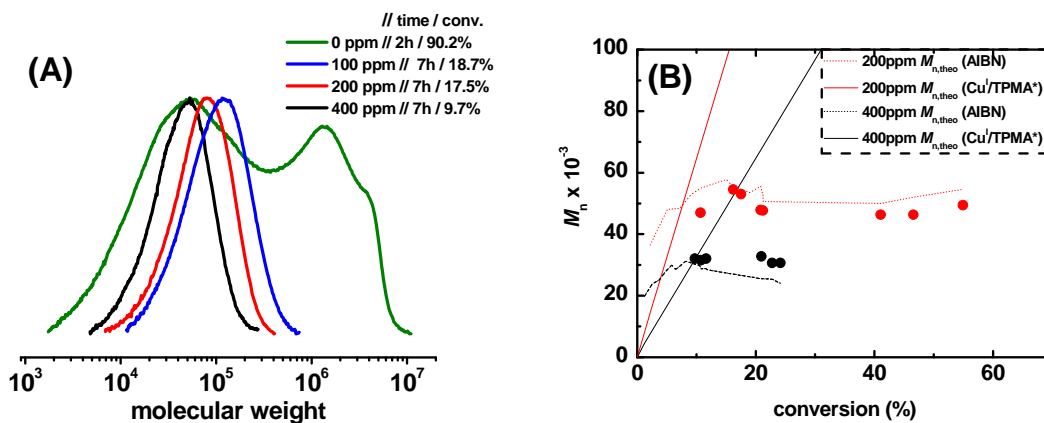
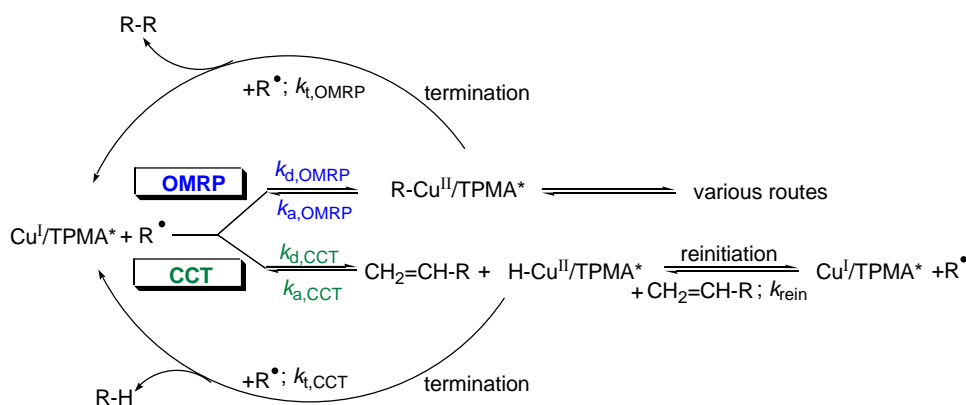


**Figure 2.** (A) Normalized GPC traces in the presence of 0, 100 ppm, 200 ppm, 400 ppm  $\text{Cu}^{\text{I}}\text{BF}_4/\text{TPMA}^*$  and (B)  $M_{n,\text{exp}}$  (dots) and  $M_{n,\text{theo}}$  (lines) as function of conversion, parameters and calculation of values for  $M_{n,\text{theo}}$  (AIBN) and  $M_{n,\text{theo}}$  ( $\text{Cu}^{\text{I}}\text{BF}_4/\text{TPMA}^*$ ) are provided in the SI: conditions;  $[\text{BA}]:[\text{AIBN}]:[\text{TPMA}^*]:[\text{Cu}^{\text{I}}(\text{CH}_3\text{CN})_4\text{BF}_4] = [160]:[0.2]:[0.06-0.24]:[0.016-0.064]$ ,  $[\text{BA}] = 5.6 \text{ M}$ , 20% (v/v) anisole,  $T = 60 \text{ }^\circ\text{C}$ .

1  
2  
3 Bimodal gel permeation chromatography (GPC) traces for polymer prepared in the  
4 conventional radical polymerization reactions were observed (Fig. 2A; SI, Table S3). They could  
5 be explained by an initial rapid exothermic polymerization and a two stage process. First, a high  
6 molecular weight fraction could be quickly formed in a concentrated monomer solution ( $M_n = 8$   
7  $\times 10^5 - 1 \times 10^6$ ). Then, due to the polymerization exothermicity, the temperature could increase,  
8 accelerating AIBN decomposition and resulting in a lower molecular weight fraction ( $M_n \sim 2 \times$   
9  $10^4$ ). A temperature probe directly inserted into the reaction mixture showed a temperature  
10 increase by  $>50^\circ\text{C}$  during the polymerization (SI, Fig. S5). Increasing the anisole content to 90  
11 % (v/v), slowed down the polymerization and resulted in monomodal distribution, confirming  
12 this assumption (SI, Fig. S4). The evolution of  $M_n$  and  $M_w/M_n$  with conversion in the presence of  
13  $\text{Cu}^{\text{I}}\text{BF}_4/\text{TPMA}^*$  indicated a significant differences compared to conventional RP. The GPC  
14 traces (Fig. 2A) of the polymers obtained in the reactions conducted in the presence of  
15  $\text{Cu}^{\text{I}}\text{BF}_4/\text{TPMA}^*$ , showed narrower molecular weight distributions (MWD)  $M_w/M_n \sim 1.6$  (SI, Fig.  
16 S2B). Nevertheless,  $M_{n,\text{exp}}$  did not show a linear increase with conversion (SI, Fig. S2B) and the  
17  $M_{n,\text{exp}}$  values were similar to or lower than the  $M_{n,\text{theo}}$  values, calculated from the actual number  
18 of chains generated by the decay of AIBN (SI, Fig. S3) or the amount of  $\text{Cu}^{\text{I}}\text{BF}_4/\text{TPMA}^*$ ,  
19 respectively. This could suggest the participation of a chain transfer process, although less  
20 efficient than in a typical CCT which normally gives oligomers.<sup>19a</sup>

21  
22  
23  
24  
25  
26  
27  
28  
29  
30  
31  
32  
33  
34  
35  
36  
37  
38  
39  
40  
41  
42  
43  
44  
45  
46  
47 **Potential polymerization mechanisms.** Since the radical concentration in the system with  $\text{Cu}^{\text{I}}$   
48 is much lower than the conventional RP, a radical trapping by the  $\text{Cu}^{\text{I}}\text{BF}_4/\text{TPMA}^*$  complex is  
49 likely. Since an excess of  $\text{TPMA}^*$  was used to insure efficient formation of the  $\text{Cu}^{\text{I}}\text{BF}_4/\text{TPMA}^*$   
50 complex, the ligand itself could also cause retardation. However, a blank experiment with a  
51  $[\text{TPMA}^*]:[\text{AIBN}]$  ratio of 0.24:0.2 carried out under conditions similar to those with 400 ppm of  
52  
53  
54  
55  
56  
57  
58  
59  
60

Cu<sup>I</sup>BF<sub>4</sub>/TPMA\* exhibited a conventional RP behaviour with 77% conversion after 0.5 h forming a polymer with a broad MWD. In addition, a blank experiment utilizing Cu<sup>I</sup>(CH<sub>3</sub>CN)<sub>4</sub>BF<sub>4</sub> salt (without TPMA\*) also resulted in conventional RP behaviour (72% conversion after 0.5 h with  $M_w/M_n = 13.6$ ). This indicates that only the Cu<sup>I</sup>BF<sub>4</sub>/TPMA\* complex interferes with the conventional radical chain growth process. Scheme 3 proposes two feasible pathways for the Cu-mediated reactions.



**Scheme 3.** Possible pathways during the AIBN-initiated polymerization of BA with Cu<sup>I</sup>BF<sub>4</sub>/TPMA\* (= Cu<sup>I</sup>/TPMA\*).

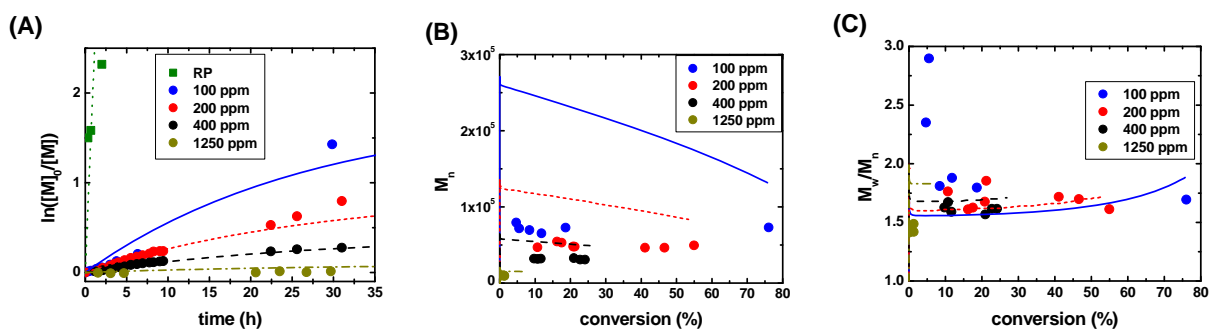
Polymerizations with different initial AIBN concentrations (SI, Fig. S6) were performed in order to define the rate determining step for both pathways. A linear dependence of  $k_{app}$  on the [AIBN] (SI, Fig. S7) was observed. As outlined in the supporting information, this linear dependence of the radical concentration and consequently the polymerization rate, is consistent with slow formation of the R-Cu<sup>II</sup> intermediates (rate-determining step) followed by fast termination reactions between the R-Cu<sup>II</sup> intermediates and the propagating radicals. In case of rapid formation of the Cu<sup>II</sup> intermediates, followed by slow termination with propagating radicals, a square root dependence of  $k_{app}$  on the [AIBN] would result.

1  
2  
3 In the OMRP scenario, polymerizations in the presence of  $\text{Cu}^{\text{I}}\text{BF}_4/\text{TPMA}^*$  are slower and,  
4 consequently, after longer reaction times, a greater number of radicals are generated from AIBN,  
5 leading to lower molecular weights. Organometallic copper(II) compounds are intrinsically  
6 unstable and therefore rarely studied,<sup>27</sup> although they were postulated as intermediates in  
7 aqueous solutions.<sup>28</sup> Decomposition of paramagnetic  $\text{R-Cu}^{\text{II}}/\text{TPMA}^*$  ( $S = 1/2$ ) might take place  
8 through termination with another radical ( $\text{R}^*$ ) to produce  $\text{R-R}$  by recombination and regenerate  
9  $\text{Cu}^{\text{I}}/\text{TPMA}^*$ . Radical-radical coupling processes were previously reported.<sup>7b, 24b</sup> This pathway is  
10 in agreement with observed  $M_w/M_n \sim 1.6$  and constant low polymerization rates. Furthermore,  
11 decomposition of  $\text{R-Cu}^{\text{II}}/\text{L}$  can occur *via* additional routes, *i.e.*: 1) a one electron reduction  
12 processes, yielding a  $\text{Cu}^{\text{I}}$  complex and a radical (OMRP reactivation), 2) heterolysis of the  
13 carbon-copper bond to give a  $\text{Cu}^{\text{II}}$  complex and saturated alkyl species (formed from the  
14 carbanion in the presence of  $\text{H}_2\text{O}$ ), 3) a reductive elimination processes (two electron reduction)  
15 yielding  $\text{Cu}(0)$ , or 4)  $\beta$ -elimination processes.<sup>28</sup> The formation of  $\text{Cu}(0)$  could be supported by  
16 the appearance of small particles in the homogenous polymerization mixture. Note, however,  
17 that  $\text{Cu}(0)$  can also result from disproportionation.  
18  
19  
20  
21  
22  
23  
24  
25  
26  
27  
28  
29  
30  
31  
32  
33  
34  
35  
36  
37

38 Another possibility is the formation of an unsaturated alkene and the paramagnetic copper(II)  
39 hydride ( $S = 1/2$ ),  $\text{H-Cu}^{\text{II}}/\text{TPMA}^*$ . The latter can terminate with another radical or reinitiate  
40 polymerization with another monomer. Reinitiation would start a CCT polymerization similar to  
41 that known for the cobalt/methacrylate systems.<sup>11</sup> However, the formation of polymers with  
42 relatively high molecular weights suggest that the copper hydride intermediate undergoes  
43 catalytic radical termination (CRT) with another radical, rather than reinitiation.  
44  
45  
46  
47  
48  
49  
50  
51

52 **PREDICI<sup>®</sup> simulations.** PREDICI<sup>®</sup> simulations were performed for the two most likely  
53 scenarios in order to get further insights into the potential polymerization mechanisms, cf. SI for  
54 conditions. First, the OMRP process was considered. Note that, with only deactivation taking  
55  
56  
57  
58  
59  
60

place, OMRP shows no sustained retardation; the simulations are supplied in the SI (Fig. S8). OMRP including deactivation and termination was simulated ( $k_{d,OMRP} = 1.6 \times 10^5 \text{ M}^{-1} \text{ s}^{-1}$ ,  $k_{t,OMRP} = 3 \times 10^8 \text{ M}^{-1} \text{ s}^{-1}$ , Fig. 3A-C) and the observed retardation agrees well with the experimental data. Furthermore, polymerizations were slow and depended on the amount of  $\text{Cu}^{\text{I}}\text{BF}_4/\text{TPMA}^*$  added to the reaction, while the  $M_w/M_n$  values were  $\sim 1.5$ . Similarly, CRT ( $k_{d,CRT} = 1.6 \times 10^5 \text{ M}^{-1} \text{ s}^{-1}$ ,  $k_{t,CRT} = 3 \times 10^8 \text{ M}^{-1} \text{ s}^{-1}$ ) was considered (Fig. 3D-E). The presence of transfer reactions did not alter the simulated kinetics and molecular weights were in agreement with the experimentally observed values. However, the  $M_w/M_n$  values did not decrease below  $\sim 2$ . Note that the simulations in Fig. 3 D-F are indistinguishable from a pathway resulting in an initial formation of the  $\text{R-Cu}^{\text{II}}/\text{TPMA}^*$  organometallic species. This could be followed by rapid  $\beta$ -elimination to give  $\text{H-Cu}^{\text{II}}/\text{TPMA}^*$  and an unsaturated chain, and finally a rapid termination between radicals and the  $\text{H-Cu}^{\text{II}}/\text{TPMA}^*$  to give a dead chain and  $\text{Cu}^{\text{I}}/\text{TPMA}^*$  (SI, Fig. S9), assuming  $k_{d,OMRP} = 1.6 \times 10^5 \text{ M}^{-1} \text{ s}^{-1}$ ,  $k_{\beta} = 3 \times 10^8 \text{ s}^{-1}$ ,  $k_{t,CRT} = 3 \times 10^8 \text{ M}^{-1} \text{ s}^{-1}$ . The concentrations of the various Cu species under the OMRP or the CRT conditions are given in the SI (Fig. S10). In all cases,  $\text{Cu}^{\text{I}}$  concentrations are constant throughout the reaction, and  $[\text{Cu}^{\text{II}}]$  is very low ( $\sim 1 \mu\text{M}$ ), since the reaction between  $\text{Cu}^{\text{I}}$  and the propagating radical is the rate limiting step.



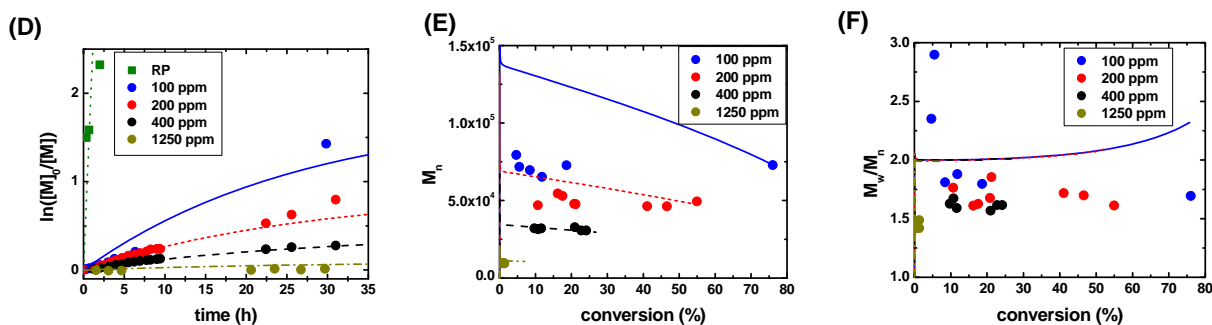


**Figure 3.** Superposition of simulated (lines) and experimental (circles) data for the polymerization of BA at various  $[\text{Cu}^{\text{I}}]$  loadings: green, 0 ppm (conventional radical polymerization); blue, 100 ppm; red, 200 ppm; black, 400 ppm; brown, 1250 ppm. (A-C) OMRP with deactivation and termination ( $k_{\text{d,OMRP}} = 1.6 \times 10^5 \text{ M}^{-1} \text{ s}^{-1}$ ,  $k_{\text{t,OMRP}} = 3 \times 10^8 \text{ M}^{-1} \text{ s}^{-1}$ ): (A) Kinetic plots, (B)  $\text{DP}_n$  and (C)  $M_w/M_n$  vs. conversion; (D-F) Catalytic radical termination (CRT) ( $k_{\text{d,CRT}} = 1.6 \times 10^5 \text{ M}^{-1} \text{ s}^{-1}$ ,  $k_{\text{t,CRT}} = 3 \times 10^8 \text{ M}^{-1} \text{ s}^{-1}$ ): (A) Kinetic plots (B),  $\text{DP}_n$  and (C)  $M_w/M_n$  vs. conversion; conditions:  $[\text{BA}]:[\text{AIBN}]:[\text{Cu}^{\text{I}}/\text{TPMA}^*] = [160]:[0.2]:[0.016-0.2]$ ,  $[\text{BA}] = 5.6 \text{ M}$ ,  $T = 60 \text{ }^\circ\text{C}$ . Points refer to experimental data, lines refer to kinetic simulations.

**Consequences for ATRP:** Under the same conditions (temperature,  $[\text{AIBN}]$ ,  $[\text{Cu}]$ ), the polymerization is much faster in the presence of RBr (ICAR ATRP). With 100 ppm  $\text{Cu}^{\text{I}}\text{BF}_4/\text{TPMA}^*$ , the apparent rate constant is  $k_{\text{app},100\text{ppm}} = 0.048 \text{ h}^{-1}$  and in the presence of 100 ppm  $\text{Cu}^{\text{II}}\text{Cl}_2/\text{TPMA}^*$  (and 0.037 M of alkyl bromide) the apparent rate constant is  $k_{\text{app},100\text{ppm}} = 0.36 \text{ h}^{-1}$ . Therefore, the contribution of interactions of radicals with  $\text{Cu}^{\text{I}}/\text{TPMA}^*$  (retardation) to the overall ICAR ATRP rate is not very significant. Consequently, one can conclude that the control observed under ATRP conditions can be assigned to the ATRP equilibrium. ICAR ATRP of BA with 100 ppm catalyst loading showed excellent agreement between  $M_{n,\text{exp}}$  and  $M_{n,\text{theo}}$ , providing polymers with low values  $M_w/M_n=1.15$ , whereas the polymerization in the presence of



1  
2  
3 Cu<sup>I</sup>BF<sub>4</sub>/TPMA\* in the absence of an ATRP initiator showed uncontrolled characteristics,  
4  
5 generating polymers with  $M_w/M_n = 1.88$  after 4 h. Indeed PREDICI<sup>®</sup> simulations show that under  
6  
7 ATRP conditions the polymerization of BA with AIBN at 60 °C is much better controlled in the  
8  
9 presence of RBr (SI, Fig. S11). The modelled system agrees well with the results of reactions  
10  
11 performed earlier for butyl acrylate. These simulations showed that in the presence of alkyl  
12  
13 halides the rate of polymerization closely matched that of the RP process, regardless of whether  
14  
15 the system was initiated in the presence of Cu<sup>I</sup> or Cu<sup>II</sup>. In both cases control over the molecular  
16  
17 weight was very good. Furthermore, inclusion of either OMRP followed by termination of the  
18  
19 organometallic species, or CRT of the Cu<sup>II</sup> hydride, into this ATRP scheme resulted in minimal  
20  
21 impact in terms of the polymerization rate or controllability. In contrast, in the absence of RBr,  
22  
23 only the OMRP or CRT pathways are possible and the rate of polymerization is decreased, as  
24  
25 well as the control over the polymerization. This difference is due to the fact that the ATRP  
26  
27 equilibrium shifts nearly all Cu<sup>I</sup> species to X-Cu<sup>II</sup>, effectively removing the majority of the Cu<sup>I</sup>  
28  
29 complex that can terminate propagating chains, from the reaction medium. However, due to the  
30  
31 high activity of the TPMA\* based catalyst complexes, the minute amounts of Cu<sup>I</sup>, are still very  
32  
33 active in ATRP, and the low mole fractions are sufficient for the continuous reactivation of  
34  
35 dormant species.  
36  
37  
38  
39  
40  
41  
42  
43  
44

45 **Comparison with previously observed interactions with Cu/dTbpy and Cu/dNbpy:** The  
46  
47 AIBN-initiated polymerization of MA in the presence of Cu<sup>I</sup>OTf/dTbpy reduced the  
48  
49 polymerization rates.<sup>23</sup> While the polymerization conditions used in the present work were  
50  
51 similar to those of the previous report (for a detailed comparison, see SI Table S4), there was a  
52  
53 much larger decrease in the polymerization rate for a polymerization of BA ( $k_p, 60^\circ\text{C} = 33700$   
54  
55  $\text{Lmol}^{-1}\text{s}^{-1}$ )<sup>29</sup> conducted in the presence of Cu<sup>I</sup>BF<sub>4</sub>/TPMA\* (8.5% conversion after 3 h ) than for  
56  
57  
58  
59  
60

1  
2  
3 the polymerization of MA ( $k_p, 60^\circ\text{C} = 33100 \text{ Lmol}^{-1}\text{s}^{-1}$ )<sup>29</sup> in the presence of Cu<sup>I</sup>OTf/dTbpy (~35%  
4 conversion after 3 h), although solvent effects can also have some contributions.<sup>15d</sup> There were  
5 also significant differences in the resulting  $M_n$  and  $M_w/M_n$  values. While the  $M_n$  values for the  
6 PMA polymers formed in the presence of the Cu<sup>I</sup>OTf/dTbpy complex were  $\sim 2 \times 10^5$ , the PBA  
7 polymers obtained in the presence of Cu<sup>I</sup>BF<sub>4</sub>/TPMA\* had  $M_n$  values  $\sim 3 \times 10^4$ . These results  
8 suggest that the substantially more reducing and more active Cu<sup>I</sup>BF<sub>4</sub>/TPMA\* ATRP catalyst  
9 interacts with the growing acrylate radicals stronger than the less active Cu<sup>I</sup>OTf/dTbpy complex.  
10  
11  
12  
13  
14  
15  
16  
17  
18  
19  
20  
21

22 **Conclusions:** Interactions between radicals and highly active ATRP complexes  
23 (Cu<sup>I</sup>BF<sub>4</sub>/TPMA\*) were observed in the polymerization of acrylates. These interactions led to  
24 significantly slower polymerizations, lower molecular weights and narrower molecular weight  
25 distributions. This suggests that OMRP trapping processes contribute to retarding the  
26 polymerization and preventing the initial formation of polymers with very high molecular  
27 weights. Furthermore, the experiments described here also demonstrate the existence of  
28 additional termination processes, in the presence of the Cu<sup>I</sup>BF<sub>4</sub>/TPMA\* complex, that ultimately  
29 quench the free radicals generated by excess AIBN. These reactions may include radical addition  
30 to the OMRP dormant species R-Cu<sup>II</sup>/TPMA\*, to generate R-R coupling products, and/or  
31 addition to the H-Cu<sup>II</sup>/TPMA\* hydride intermediate of a CRT process to generate R-H, as shown  
32 in Scheme 3. PREDICI simulations confirmed the possibility of R-Cu<sup>II</sup>/TPMA\* or H-  
33 Cu<sup>II</sup>/TPMA\* formation, followed by a termination reaction with another radical to give  
34 Cu<sup>I</sup>/TPMA\* and the recombination product. Further investigations are planned to elucidate this  
35 mechanistic question. Nevertheless, in the presence of ATRP initiators, the ATRP equilibrium is  
36 primarily responsible for exercising control over the polymerization procedure and dominates  
37 over the OMRP processes.  
38  
39  
40  
41  
42  
43  
44  
45  
46  
47  
48  
49  
50  
51  
52  
53  
54  
55  
56  
57  
58  
59  
60

## ASSOCIATED CONTENT

**Supporting Information.** “This material is available free of charge via the Internet at <http://pubs.acs.org>.”

## AUTHOR INFORMATION

**Corresponding Author**

\* Email: km3b@andrew.cmu.edu.

**Author Contributions**

The manuscript was written through contributions of all authors. All authors have given approval to the final version of the manuscript.

## ACKNOWLEDGMENT

The authors would like to thank the CRP Consortium at Carnegie Mellon University and NSF (CHE-1026060, CHE-1039870, CHE-0130903) for financial support and Dr. Johannes Buback for his help with the stopped-flow measurements. K.S. thanks the Deutsche Forschungsgemeinschaft (DFG) for her postdoctoral fellowship (SCHR 1314). R.P thanks the Agence National de la Recherche (project OMRP, grant ANR 2010 BLANC 7101).

## REFERENCES

1. (a) Matyjaszewski, K.; Davis, T. P., *Handbook of Radical Polymerization*. Wiley-Interscience: Hoboken, **2002**; p 936 pp;(b) Moad, G., Radical Polymerization in *Polymer Science: A Comprehensive Reference*, Matyjaszewski, K.; Möller, M., Eds. Elsevier: Amsterdam, **2012**; Vol. 3, pp 59.
2. Jenkins, A. D.; Jones, R. G.; Moad, G. *Pur. Appl. Chem.* **2010**, 82, 483.

3. (a) Coessens, V.; Pintauer, T.; Matyjaszewski, K. *Prog. Polym. Sci.* **2001**, *26*, 337;(b) Matyjaszewski, K.; Davis, K. A., *Statistical, Gradient and Segmented Copolymers by Controlled/Living Radical Polymerizations*. Springer Verlag: Berlin, **2002**; p 203 pp;(c) Tsarevsky, N. V.; Matyjaszewski, K. *Chem. Rev.* **2007**, *107*, 2270;(d) Matyjaszewski, K.; Tsarevsky, N. V. *Nat. Chem.* **2009**, *1*, 276;(e) Wang, Y.; Matyjaszewski, K. *Macromolecules* **2011**, *44*, 1226;(f) Matyjaszewski, K. *Macromolecules* **2012**, *45*, 4015.
4. di Lena, F.; Matyjaszewski, K. *Prog. Polym. Sci.* **2010**, *35*, 959.
5. (a) Poli, R. *Angew. Chem. Int. Ed.* **2006**, *45*, 5058;(b) Poli, R., Organometallic Mediated Radical Polymerization in *Polymer Science: A Comprehensive Reference*, Matyjaszewski, K.; Möller, M., Eds. Elsevier BV: Amsterdam, **2012**; Vol. 3, pp 351.
6. Wayland, B. B.; Poszmik, G.; Mukerjee, S. L.; Fryd, M. *J. Am. Chem. Soc.* **1994**, *116*, 7943.
7. (a) Smith, K. M.; McNeil, W. S.; Abd-El-Aziz, A. S. *Macromol. Chem. Phys.* **2010**, *211*, 10;(b) Poli, R. *Eur. J. Inorg. Chem.* **2011**, *2011*, 1513;(c) Hurtgen, M.; Detrembleur, C.; Jerome, C.; Debuigne, A. *Polym. Rev.* **2011**, *51*, 188;(d) Allan, L. E. N.; Perry, M. R.; Shaver, M. P. *Prog. Polym. Sci.* **2012**, *37*, 127.
8. (a) Maria, S.; Kaneyoshi, H.; Matyjaszewski, K.; Poli, R. *Chem.-Eur. J.* **2007**, *13*, 2480;(b) Santhosh, K.; Gnanou, Y.; Champouret, Y.; Daran, J.-C.; Poli, R. *Chem.-a Eur. J.* **2009**, *15*, 4874.
9. Zhao, Y.; Dong, H.; Li, Y.; Fu, X. *Chem. Commun.* **2012**, *48*, 3506.
10. Debuigne, A.; Morin, A. N.; Kermagoret, A.; Piette, Y.; Detrembleur, C.; Jérôme, C.; Poli, R. *Chem. – Eur. J.* **2012**, DOI: 10.1002/chem.201201456.
11. Heuts, J. P. A.; Forster, D. J.; Davis, T. P.; Yamada, B.; Yamazoe, H.; Azukizawa, M. *Macromolecules* **1999**, *32*, 2511.
12. (a) Wang, J.-S.; Matyjaszewski, K. *J. Am. Chem. Soc.* **1995**, *117*, 5614;(b) Matyjaszewski, K.; Xia, J. *Chem. Rev.* **2001**, *101*, 2921;(c) Matyjaszewski, K.; Spanswick, J. In: *Matyjaszewski K and Möller M (eds.) Polymer Science: A Comprehensive Reference* **2012**, Vol. 3, 377.
13. (a) Jakubowski, W.; Matyjaszewski, K. *Angew. Chem. Int. Ed.* **2006**, *45*, 4482;(b) Magenau, A. J. D.; Strandwitz, N. C.; Gennaro, A.; Matyjaszewski, K. *Science* **2011**, *332*, 81.
14. Matyjaszewski, K.; Jakubowski, W.; Min, K.; Tang, W.; Huang, J.; Braunecker, W. A.; Tsarevsky, N. V. *Proc. Natl. Acad. Sci. USA* **2006**, *103*, 15309.

- 1  
2  
3  
4  
5  
6  
7  
8  
9  
10  
11  
12  
13  
14  
15  
16  
17  
18  
19  
20  
21  
22  
23  
24  
25  
26  
27  
28  
29  
30  
31  
32  
33  
34  
35  
36  
37  
38  
39  
40  
41  
42  
43  
44  
45  
46  
47  
48  
49  
50  
51  
52  
53  
54  
55  
56  
57  
58  
59  
60
15. (a) Tang, W.; Matyjaszewski, K. *Macromolecules* **2006**, *39*, 4953;(b) Tang, W.; Matyjaszewski, K. *Macromolecules* **2007**, *40*, 1858;(c) Seeliger, F.; Matyjaszewski, K. *Macromolecules* **2009**, *42*, 6050;(d) Braunecker, W. A.; Tsarevsky, N. V.; Gennaro, A.; Matyjaszewski, K. *Macromolecules* **2009**, *42*, 6348;(e) Morick, J.; Buback, M.; Matyjaszewski, K. *Macromol. Chem. Phys.* **2011**, *212*, 2423.
16. Tang, W.; Kwak, Y.; Braunecker, W.; Tsarevsky, N. V.; Coote, M. L.; Matyjaszewski, K. *J. Am. Chem. Soc.* **2008**, *130*, 10702.
17. Magenau, A. J. D.; Kwak, Y.; Schröder, K.; Matyjaszewski, K. *ACS Macro Lett.* **2012**, 508.
18. Schröder, K.; Mathers, R. T.; Buback, J.; Konkolewicz, D.; Magenau, A. J. D.; Matyjaszewski, K. *ACS Macro Lett.* **2012**, *1*, 1037.
19. (a) Le Grogne, E.; Claverie, J.; Poli, R. *J. Am. Chem. Soc.* **2001**, *123*, 9513;(b) Stoffelbach, F.; Poli, R.; Maria, S.; Richard, P. *J Organomet Chem* **2007**, *692*, 3133.
20. Braunecker, W. A.; Itami, Y.; Matyjaszewski, K. *Macromolecules* **2005**, *38*, 9402.
21. Shaver, M. P.; Allan, L. E. N.; Gibson, V. C. *Organometallics* **2007**, *26*, 4725.
22. Allan, L. E. N.; MacDonald, J. P.; Reckling, A. M.; Kozak, C. M.; Shaver, M. P. *Macromol. Rapid Commun.* **2012**, *33*, 414.
23. Matyjaszewski, K.; Woodworth, B. E. *Macromolecules* **1998**, *31*, 4718.
24. (a) Kinoshita, I.; James Wright, L.; Kubo, S.; Kimura, K.; Sakata, A.; Yano, T.; Miyamoto, R.; Nishioka, T.; Isobe, K. *Dalton Trans.* **2003**, 1993;(b) Goj, L. A.; Blue, E. D.; Delp, S. A.; Gunnoe, T. B.; Cundari, T. R.; Petersen, J. L. *Organometallics* **2006**, *25*, 4097.
25. Fischer, H.; Radom, L. *Angew. Chem. Int. Ed.* **2001**, *40*, 1340.
26. Tang, W.; Tsarevsky, N. V.; Matyjaszewski, K. *J. Am. Chem. Soc.* **2006**, *128*, 1598.
27. Jastrzebski, J. T. B. H.; van Koten, G., Structures and Reactivities of Organocopper Compounds in *Modern Organocopper Chemistry*, Krause, N., Ed. *WILEY-VCH*: Weinheim, **2002**.
28. (a) Navon, N.; Golub, G.; Cohen, H.; Meyerstein, D. *Organometallics* **1995**, *14*, 5670;(b) Navon, N.; Cohen, H.; Meyerstein, D. *Inorg. Chem.* **1997**, *36*, 3781.
29. Buback, M.; Kurz, C. H.; Schmaltz, C. *Macromol. Chem. Phys.* **1998**, *199*, 1721.

1  
2  
3  
4  
5  
6 Table of Contents graphic.  
7  
8  
9  
10  
11  
12  
13  
14  
15  
16  
17  
18  
19  
20  
21  
22  
23  
24  
25  
26  
27  
28  
29  
30  
31  
32  
33  
34  
35  
36  
37  
38  
39  
40  
41  
42  
43  
44  
45  
46  
47  
48  
49  
50  
51  
52  
53  
54  
55  
56  
57  
58  
59  
60

